Parametric Study of Food Can Corrugation Geometry by using Finite Element Method

Rattharong Rotbunsongsri[1], Pattaramon Jongpradist[*1] and Thoatsanope Kamnerdtong[1]
[1]Department of Mechanical Engineering, King Mongkut's University of Technology Thonburi
Bangkok, Thailand 10140
*Corresponding Author: Tel: 02 470 9124, Fax: 02 470 9111,
E-mail: pattaramon.tan@kmutt.ac.th

Abstract

Food cans are usually manufactured as a cylindrical thin shell because the shape is easy to form and the material cost is economized. However, the performance of thin circular shells under combined loading is not high especially when subjected to bending stresses. Corrugated can wall is designed to stiffen the can body such that it can endure loadings occurring in the manufacturing process. On the other hand, the corrugation causes decrease in the axial load capacity of the can. A proper design and dimensions of food can corrugation to minimize the material cost whereas the structural performances of the can are not compromised is necessary. In the present work, Finite Element Method (FEM) is employed to study the effects of corrugation geometries to a commercial food can. The 603x700 commercial food can is examined. The parameters of interest include the radius, spacing, number and depth of corrugation. The effects of changing each geometric parameter to the loading capacity of the can are investigated. Two-level full factorial design is employed to analyze the effects of all variables on vacuum pressure and axial load. It was found that the key parameters to the structural performances of the container for both loadings are the corrugation depth, spacing and radius. The corrugation depth has the most effect for both loadings while the number of corrugations is shown to be an insignificant factor.

***Keywords**:* Corrugation, Cylindrical shell, Food container, Finite Element Method, Buckling load.

1. Introduction

Food container industry has grown up rapidly with increasing number of population and diversity of food demand due to ability to preserve food and convenience in distribution from place to place. Metal cylindrical food can is widely used because its forming process is easy and economized. Food can design has been developed such that its strength performance is satisfied while the material used is minimized. Several designs have been done on the can's shape, corrugation, material, forming method, etc.

Theppankulngam et. al [1] studied strengths of the can structure exposed to three loadings that occurs in the manufacturing process of food containers, i.e., internal pressure, vacuum pressure and axial compressive load. High temperature and pressure generated inside the can in sterilization process was found to initiate expansion and swelling of the can lids. Vacuum pressure during food containing process causes buckling of the can body. Excessive axial load from transportation and storage also results in can buckling. Experiments as well as finite element analysis of the can under these types of loading had been performed and compared.

Wang [2] analyzed effects of the can body thickness and corrugation depth to axial load and vacuum pressure by using finite element analysis. It was shown that increase in can body thickness improved both performances. However, larger corrugation depths increased the can strength under vacuum pressure while decreased the axial load resistance.

Yamazaki [3] utilized an optimization technique to design the lightest beverage can end. Geometric parameters of the end shell were selected as parameters of variation. Finite element method was employed to simulate deforming behavior and buckling strength. Response Surface Approximation is used to optimize all variables. The weight of the proposed model was reduced by 3% when compared with that of the original model.

Xu et. al [4] applied a mathematical method in a symplectic space to obtain the solutions for dynamic buckling of cylindrical shells under impacts of axial load. Numerical examples showing phenomena of axisymmetric and non-axisymmetric buckling modes are presented.

This research focuses on the effects of corrugation design on the can body to the structural performances under vacuum pressure and axial load. The can performances and behaviors are obtained by using a finite element analysis (FEA) program, Abaqus [5] and validated with experimental results from [1]. Parametric study to determine the key factors influencing the can strength is performed by two-level full factorial design. The parameters included in this study are spacing, depth, radius, and number of corrugation.

2. Can Modeling

In this work, a commercial food can of the size 603x700 (6-3/16 inch (177 mm) high and 7 inch (153 mm) in diameter) with 17 beadings is analyzed. The can body thickness is 0.25 mm and the lid thickness is 0.28 mm.

The finite element model is shown in Fig. 1. This model uses two types of elements, i.e., 8-node reduced integration shell (S8R) and 20-node brick (C3D20) elements. The can body and can lids are meshed by 7680 and 4000 elements by using S8R. The seam between the body and each lid is meshed into 320 C3D20 elements.

The can is made of tin-coated cold-formed sheet metal. Mechanical properties of the can plates corresponding to its thickness are shown in Table. 1.

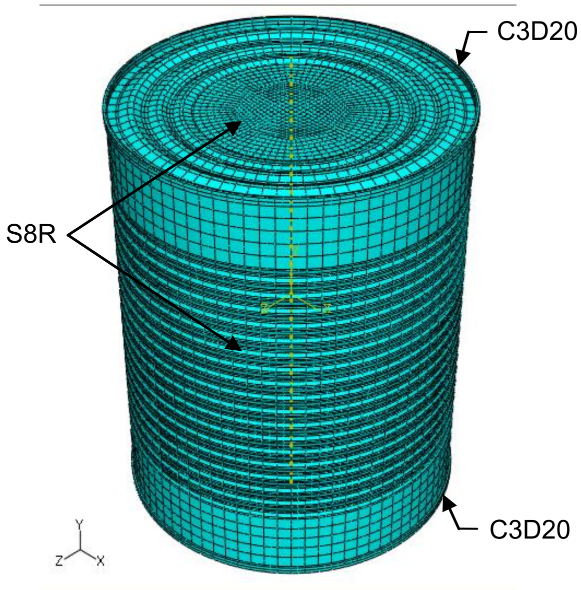

Fig. 1 Meshing model

Table. 1 Mechanical properties for different plate thicknesses

Plate thickness (mm)	Young's Modulus (GPa)	Poisson ratio	Yield strength (MPa)
0.25	219.86	0.3	456.74
0.28	229.79	0.3	426.29

3. Analysis and Validation

3.1 Loadings and Boundary Conditions

In this study, the can body structure is studied under vacuum pressure and axial compressive load. For vacuum pressure, the boundary conditions are as shown in Fig. 2a. The center of the bottom can lid is fixed from moving in all directions. The center of the top lid is restraint from moving in 1-3 plane whereas its displacement in the axial direction of the can is allowed. Vacuum load is applied as pressure on all the inside surface of the can (Fig. 2b).

For compressive load, the boundary and loading conditions are shown in Fig. 3. Two rigid plates are modeled at the top and bottom of the can to simulate the condition during the test. In this case, the same boundary conditions as those for vacuum pressure case are set but they are applied to the plate instead of the can lids (Fig. 3a). The axial load is applied as a concentrated compressive force perpendicular to the top plate as depicted in Fig. 3b.

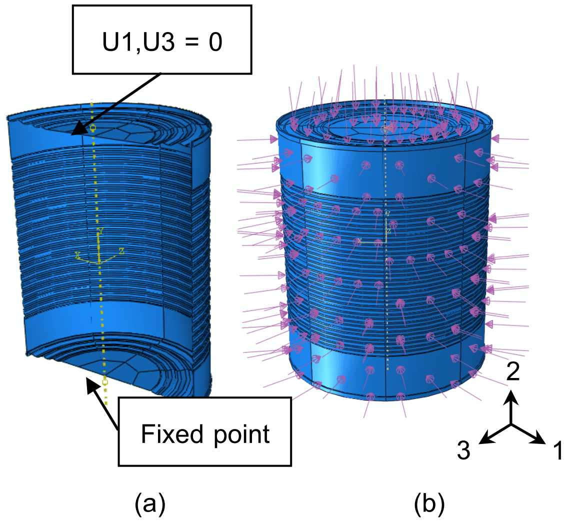

Fig. 2 (a) Boundary and (b) loading conditions for vacuum pressure

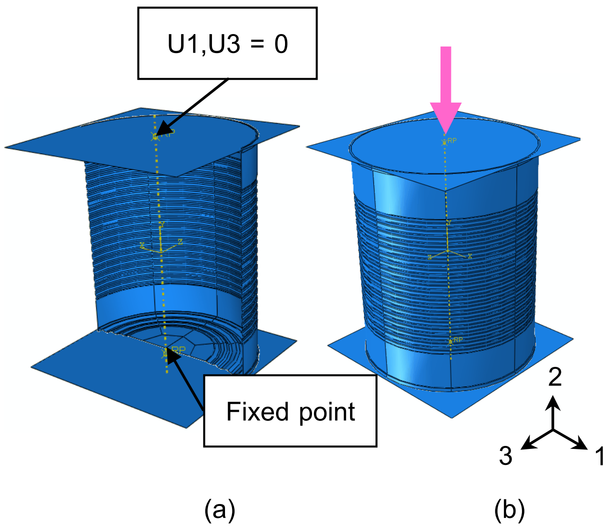

Fig. 3 (a) Boundary and (b) loading conditions for axial load

3.2 Analysis

The structural performance of the can body under vacuum pressure is analyzed by linear perturbation buckling analysis. Buckling loads and mode shapes of the can are then examined. The post-buckling behavior and strength of the can under axial compressive load obtained by first performing a linear perturbation buckling analysis and then the Riks method is employed to calculate the ultimate strength of the can. However, the post-buckling strength of thin shells under axial load is highly sensitive to imperfection of the structure. Therefore, the imperfection of the can body is determined by comparison of the experimental and FEA results. It was found that the imperfection size equal to 10% thickness gives comparable results the strengths from experiment and FEA are compared for both cases as shown in Table. 2.

The buckling pressures from FEA and experiment are 129 and 125 kPa, respectively. The buckling mode shapes for the two cases are resembled as illustrated in Fig. 4.

Table. 2 Comparison between results from finite element analysis and experiment

Results	Finite Element Analysis	Experiment	Difference (%)
Vacuum pressure (kPa)	129	125	3.2
Axial load (N)	10467	9984	5.9

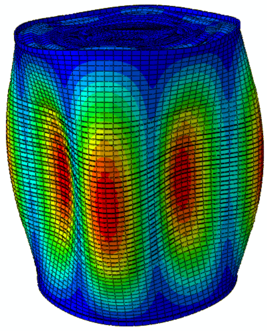

(a)

(b)

Fig. 4 Buckling mode shape under vacuum pressure from (a) FEA (b) experiment

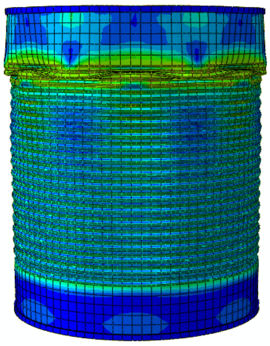

(a)

(b)

Fig. 5 Post-buckling deformation under axial load from (a) FEA (b) experiment

In the case of axial compressions, the buckling load from FEA is 10467 N while that from experiment is 9984 N. The post-buckling shapes of the can under compression are also similar as shown in Fig. 5.

4. Parametric Study of Corrugation Geometry

In this section, two-level full factorial design is used to design the can corrugation so as to find key parameters affecting the structural strength of the can under vacuum pressure and axial load. Four parameters are considered including spacing of corrugation (*S*), radius of corrugation (*R*), depth of corrugation (*D*), and number of corrugation (*N*) as depicted in Fig. 6.

In the analysis, two values (high and low) are used for each parameter. For full factorial design, all alternate cases for analysis points must be evaluated. Thus, the total number of runs is sixteen. From manufacturing limitation, the spacing is varied between 6.5 and 8 mm, the radius of corrugation between 2 and 3.5 mm, the depth 0.4-0.75, and the number of corrugation is from 15 to 17. All analysis points and responses are listed in Table. 4. It can be seen from Table. 4 that from geometric change of the corrugation vacuum and axial load, resistance of the can varied considerable up to 85.9% and 62.2% differences.

Table. 4 full factorial design

Analysis points	*S* (mm)	*R* (mm)	*D* (mm)	*N*	Vacuum pressure (kPa)	Axial load (N)
1	6.5	2	0.4	15	82.8	14598
2	8	2	0.4	15	79.9	14584
3	6.5	3.5	0.4	15	83.3	14327
4	8	3.5	0.4	15	80.4	14317
5	6.5	2	0.75	15	131.9	9288
6	8	2	0.75	15	122.7	9288
7	6.5	3.5	0.75	15	144.6	9086
8	8	3.5	0.75	15	129.0	9123
9	6.5	2	0.4	17	84.2	14600
10	8	2	0.4	17	81.7	14742
11	6.5	3.5	0.4	17	85.7	14484
12	8	3.5	0.4	17	82.1	14507
13	6.5	2	0.75	17	135.5	9289
14	8	2	0.75	17	125.9	9325
15	6.5	3.5	0.75	17	148.5	9188
16	8	3.5	0.75	17	132.2	9126

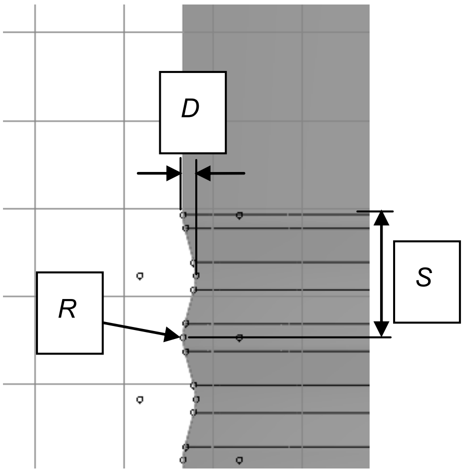

Fig. 6 Variable parameters

5. Results and Discussions

When the main effects are plotted for vacuum pressure and axial load, it can be clearly seen that the depth of corrugation has the most prominent effect to both responses. However, larger corrugation depth results in increase of the vacuum strength while the axial strength decreases as shown in Figs. 7 and 8.

Large spacing of corrugation decreases both vacuum pressure and axial strength whereas a larger number of corrugation increases both strengths. Small radius of corrugation benefits the can's performance under vacuum pressure but results in a slightly smaller resistance against axial load.

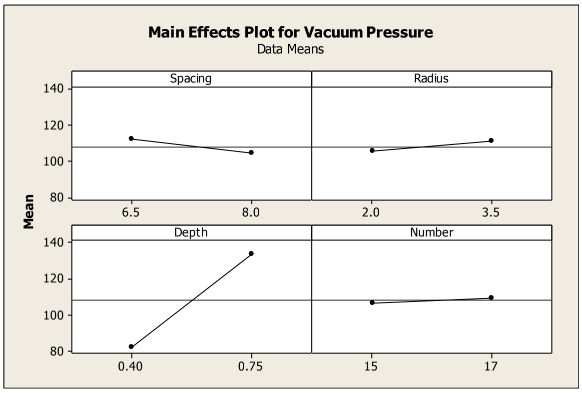

Fig. 7 Main effects plot for vacuum pressure

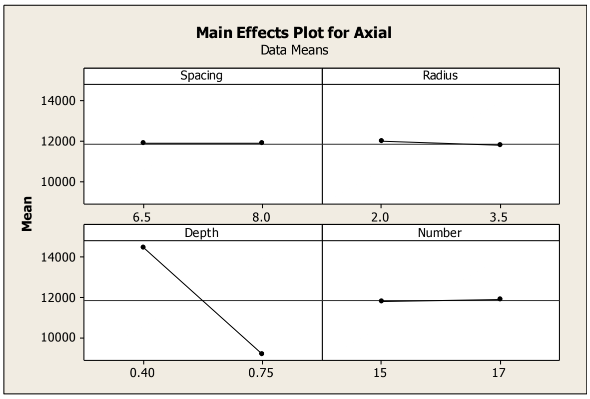

Fig. 8 Main effects plot for axial load

The normal probability plot of the effects for vacuum pressure (Fig. 9) shows the main of all variables and interaction effects. The depth of corrugation shows much more significant effect than other parameters. The other significant effects are spacing, radius, interaction between spacing and depth, and interaction between radius and depth. It is noticed that the number of corrugation both the main and interaction effects are insignificant for vacuum pressure. The values of the effects and coefficients for vacuum pressure are shown in Table. 5.

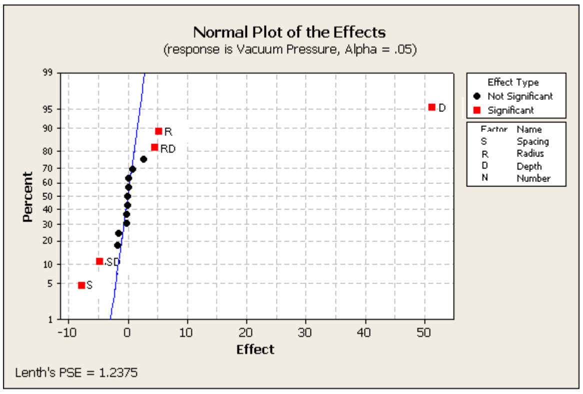

Fig. 9 Normal plot of vacuum pressure

For axial load, the normal probability plot (Fig. 10) of the effects indicates that only the main effects from the depth and radius of corrugation, both in negative field, are the significant parameters. The effect from the depth is evidently the most important. All effects and coefficients of the four variables and their interactions for axial load are shown in Table. 6.

Table. 5 Effects for vacuum pressure

Term	Effect	Coefficient
Constant		108.2
S	-7.8	-3.9
R	5.2	2.6
D	51.3	25.6
N	2.7	1.3
*S*R*	-1.8	-0.9
*S*D*	-4.9	-2.4
*S*N*	-0.2	-0.1
*R*D*	4.4	2.2
*R*N*	0.2	0.1
*D*N*	0.8	0.4
*S*R*D*	-1.5	-0.8
*S*R*N*	-0.2	-0.1
*S*D*N*	-0.1	-0.05
*R*D*N*	-0.1	-0.05
*S*R*D*N*	0.1	0.05

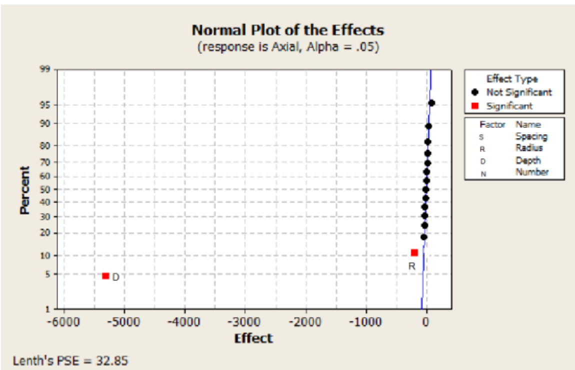

Fig. 10 Normal plot of axial load

Table. 6 Effects for axial load

Term	Effect	Coefficient
Constant		11867
S	19	10
R	-194	-97
D	-5306	-2653
N	81	41
*S*R*	-22	-11
*S*D*	-16	-8
*S*N*	16	8
*R*D*	28	14
*R*N*	32	16
*D*N*	-46	-23
*S*R*D*	7	3
*S*R*N*	-32	-16
*S*D*N*	-32	-16
*R*D*N*	-15	-7
*S*R*D*N*	-1	-1

These results can be further used in the optimization of the can corrugation depending on the performance requirement of the can structure. However, the number of corrugation can be excluded from consideration since its effects on the strengths for both cases are insignificant.

6. Conclusions and Recommendations

This research employs finite element analysis to analyze the effects of food can corrugation to the can structural performances under vacuum pressure and axial compressive load. Full factorial design is used to determine the main and interaction effects of four geometric parameters on each response. It was found that the depth of corrugation has the most effects for both load cases. Spacing and radius are also shown to be significant while the effect from the number of the corrugation is insignificant. The key parameters can be further applied to response surface methodology so as to design an optimized corrugation shape for each loading condition.

7. Acknowledgement

Financial support from Thailand Research Fund (TRF) under grant MRG5380005 is gratefully acknowledged.

8. References

[1] Theppankulngam, P., Jongpradist, P. and Kamnerdtong, T. (2008). Study of Loading Capacity of Corrugated Food Cans Using Finite Element Method, paper presented in *The 22nd Conference of Mechanical Engineering Network of Thailand*, Thammasat University, Rangsit Campus, Pathumthani, Thailand.

[2] Wang, J. (2001), Design optimization of rigid metal containers, *Finite Elements in Analysis and Design*, Vol.37, 2001, pp. 273-286.

[3] Yamazaki, K., Itoh, R., Watanabe. M., Han, J. and Nishiyama, S. (2007). Applications of Structural Optimization Techniques in Light Weighting of Aluminum Beverage Can Ends. *Journal of Food Engineering*, Vol.81, 2007, pp. 341-346.

[4] Xu, X., Ma, Y., C.W. L. and Chu, H. (2006). Dynamic buckling of cylindrical shells subject to an axial impact in a symplectic system, *International Journal of Solids and Structures*, Vol.43, 2006, pp.3905-3919.

[5] Dassault Systemer Simulia Corp. (2008). Abaqus Theory Manual, Version 6.8, Providence, RI, USA.